Defect Disorder of Titanium Dioxide

T. Bak, J. Nowotny,* and M. K. Nowotny

Centre for Materials Research in Energy Conversion, School of Materials Science and Engineering, University of New South Wales, Sydney, NSW 2052, Australia

Received: June 14, 2006; In Final Form: August 24, 2006

The present work derived defect disorder diagram representing the effect of oxygen activity on the concentration of both ionic and electronic defects for undoped TiO_2. This diagram was determined using the equilibrium constants derived in the present work, including (i) the intrinsic electronic equilibrium constant, (ii) the equilibrium constant for the formation of oxygen vacancies, and (iii) equilibrium constant for the formation of titanium vacancies. These equilibrium constants are consistent with three properties determined independently, including: electrical conductivity, thermoelectric power and change of mass determined by thermogravimetry. The derived defect disorder diagram may be used for tailoring semiconducting properties of TiO_2 that are desired for specific applications through the selection of optimized processing conditions.

1. Introduction

The work of Fujishima and Honda[1] showed that TiO_2 exhibits outstanding photoelectrochemical properties, which may be utilized for the conversion of solar energy into chemical energy. Specifically, they have demonstrated that TiO_2 may be used as a photoelectrode for water splitting. The discovery by Fujishima and Honda[1] resulted in an increased interest in TiO_2. The research aims at the modification of its properties in order to achieve TiO_2 with enhanced photosensitivity. It was shown that defect chemistry may be used as a framework for the modification of these properties of TiO_2 that are closely related to its photoelectrochemical properties, including electronic structure and charge transport.[2−4] In other words, defect chemistry may be used to tailor the properties of TiO_2 in order to achieve the properties that are needed for its use as a high-performance photoelectrode.

There is a close relationship between defect disorder and electrical properties in nonstoichiometric oxides.[2,5,6] Defect disorder of TiO_2 has been considered in terms of oxygen vacancies and titanium interstitials.[5] These defects, which are donors of electrons, well explain *n*-type properties of TiO_2. It has been recently shown, however, that TiO_2 is an amphoteric semiconductor that exhibits *n*-type and *p*-type properties at low and high oxygen activities, respectively.[7] These properties cannot be explained by the presence of oxygen vacancies and titanium interstitials as the only ionic defects in TiO_2.

It has also been shown that the transport of defects in TiO_2 should be considered in terms of two kinetics regimes, including the following:[8]

(1) Kinetic Regime I, in which the gas/solid equilibration is rate-controlled by the transport of fast defects, such as oxygen vacancies.

(2) Kinetics Regime II, in which the gas/solid equilibration is rate-controlled by the transport of slow defects, such as Ti vacancies.

The recently reported data of the equilibration kinetics during prolonged oxidation of TiO_2 (Kinetic Regime II) provide a strong experimental evidence of the formation and the transport of Ti vacancies.[8] Consequently, these data indicate that defect disorder of TiO_2 must be considered in terms of titanium vacancies in addition to oxygen vacancies and titanium interstitials. Recent studies by the authors have shown that the formation of Ti vacancies may lead to *p*-type conductivity at high oxygen activities.[8]

Defect chemistry of TiO_2 may be described by defect equilibria and the related equilibrium constants. The equilibrium constants reported by Kofstad[5] and Bak et al.,[9] have been used to derive defect disorder diagram of TiO_2.[10] It will be shown, however, that this defect diagram is inconsistent with the most recently reported experimental data of electrical properties for well defined (high purity) TiO_2 single crystal.[7] Therefore, there is a need to revise the defect equilibrium constants reported before in order to derive the defect disorder model that is consistent with the experimental data. This is the objective of the present work. This will be achieved by using the experimental data of several properties determined independently, including the following:

- Electrical conductivity data[7,8]
- Thermoelectric power data[8,11]
- Thermogravimetry data[12−18]

2. Defect Chemistry of TiO_2

2.1. Defect Equilibria. The defect disorder of TiO_2 depends on oxygen activity. Therefore, defect disorder models may be considered within certain oxygen activity regimes that are outlined below. These defect disorders and the related electrical properties for undoped TiO_2 may be explained in terms of three types of defects: oxygen vacancies, titanium interstitials, and titanium vacancies. Their formation may be expressed according to the following equilibria:

$$O_O \rightleftarrows V_O^{\bullet\bullet} + 2e' + \frac{1}{2}O_2 \quad (1)$$

$$2O_O + Ti_{Ti} \rightleftarrows Ti_i^{\bullet\bullet\bullet} + 3e' + O_2 \quad (2)$$

* Corresponding author phone: +61 2 9385 6465; fax: +61 2 9385 6467; e-mail: J. Nowotny@unsw.edu.au.

10.1021/jp063700k CCC: $33.50
Published on Web 10/10/2006

$$O_2 \rightleftarrows 2O_O + V_{Ti}''''+ 4h^{\bullet} \quad (3)$$

$$\text{nil} \rightleftarrows e' + h^{\bullet} \quad (4)$$

These equilibria are described by the following equilibrium constants, respectively:

$$K_1 = [V_O^{\bullet\bullet}]n^2p(O_2)^{1/2} \quad (5)$$

$$K_2 = [Ti_i^{\bullet\bullet\bullet\bullet}]n^3p(O_2) \quad (6)$$

$$K_3 = [V_{Ti}''''][p^4p(O_2)^{-1} \quad (7)$$

$$K_i = np \quad (8)$$

where n and p denote the concentrations of electrons and holes, respectively. The recently reported studies of the electrical properties of TiO_2 at elevated temperatures, including the determination of effect of oxygen activity, $p(O_2)$, on electrical conductivity and thermoelectric power,[7] indicate that the defect disorder of undoped TiO_2 may be considered within several regimes, including the following:

(1) Extremely reduced regime.
(2) Strongly reduced regime
(3) Reduced regime.
(4) Oxidation regime.

The effect of $p(O_2)$ on the concentration of ionic and electronic defects are outlined in Table 1. The effect of $p(O_2)$ on both n and p, and the related slopes of log n, p vs log $p(O_2)$, within the regimes outlined above are represented in Figure 1. As seen, the reduced and oxidation regimes require that the concentration of titanium vacancies is comparable to the concentration of oxygen vacancies.

Kofstad[5] also considers the formation of tetra-valent Ti interstitials, which are formed according to the following equilibria:

$$Ti_i^{\bullet\bullet\bullet\bullet} \rightleftarrows Ti_i^{\bullet\bullet\bullet} + e' \quad (9)$$

Therefore:

$$K_4 = \frac{[Ti_i^{\bullet\bullet\bullet}]\, n}{[Ti_i^{\bullet\bullet\bullet\bullet}]} \quad (10)$$

Derivation of defect concentration diagram based on full charge neutrality requires knowledge of the equilibrium constants. The equilibrium constants K_1, K_2, and K_4 were reported by Kofstad[12] and the equilibrium constant K_i was reported by Bak et al.[9] These constants were used for derivation of defect diagram that is shown in Figure 2 for an arbitrary concentration of acceptor-type defects at 1273 K. The following section aims at the verification of this diagram in terms of the recently reported data of both electrical properties.[7]

2.2. Defect Diagram. Figure 2 represents the defect disorder diagram for undoped TiO_2 at 1273 K according to the equilibrium constants K_1, K_2, and K_4 reported by Kofstad[12] and the equilibrium constant K_i, denoted as K_i^*, reported by Bak et al.[9] This diagram was derived at a given effective concentration of acceptors, A (defined below). In the first approximation, the parameter A in Figure *2* for high purity TiO_2 may be considered as comparable to the concentration of Ti vacancies. According to Kofstad,[5] the deviation from stoichiometry in TiO_2 at 1273 K in air is 10^{-4}. Therefore, the charge compensation for high purity TiO_2 within the reduced regime requires that the concentration of Ti vacancies is of the same order.

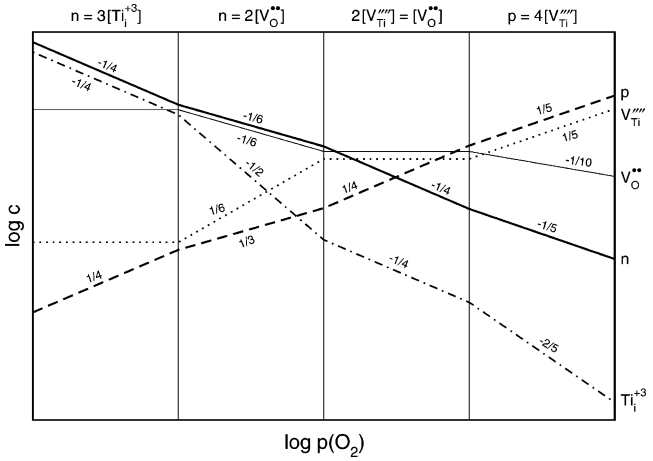

Figure 1. Defect disorder model of TiO_2 in terms of simplified charge neutrality conditions and the related concentration of ionic and electronic defects as a function of oxygen activity, $p(O_2)$.

Full charge neutrality condition requires that

$$n + [A'] + 4[V_{Ti}''''] = p + [D^{\bullet}] + 2[V_O^{\bullet\bullet}] + 3[Ti_i^{\bullet\bullet\bullet}] + 4[Ti_i^{\bullet\bullet\bullet\bullet}] \quad (11)$$

where $[A']$ and $[D^{\bullet}]$ denote the concentrations of foreign acceptors and donors, respectively. The expression (11) may be reduced to the following form:

$$n + A = p + 2[V_O^{\bullet\bullet}] + 3[Ti_i^{\bullet\bullet\bullet}] + 4[Ti_i^{\bullet\bullet\bullet\bullet}] \quad (12)$$

where

$$A = [A'] + 4[V_{Ti}''''] - [D^{\bullet}] \quad (13)$$

The term A is the effective concentration of acceptors. For high purity TiO_2 the parameter A may be considered in terms of the concentration of Ti vacancies. Then

$$[V_{Ti}''''] = \frac{A}{4} \quad (14)$$

As seen, the concentration of electrons in TiO_2 at $p(O_2) = 21$ kPa (indicated by the vertical line in Figure 2) is over 1 order of magnitude larger than that of electron holes. Extrapolation of the $p(O_2)$ dependencies of both electronic charge carriers toward larger $p(O_2)$ indicates that the $n-p$ transition could be achieved at $p(O_2) = 300$ MPa. On the other hand, however, the experimental data of both electrical conductivity[7] and thermoelectric power,[7] shown in Figure 3, indicate that the $n-p$ transition point at 1273 K (shown by the vertical line) corresponds to substantially lower $p(O_2)$ of about 16 kPa. The discrepancy between the model shown in Figure 2 and the experimental data of the electrical properties shown in Figure 3 indicates that the model requires a modification in order to adjust to the $n-p$ transition point that is in agreement with the experimental data. Since the $n-p$ transition point is mainly sensitive to the intrinsic electronic equilibrium constant, K_i, the observed discrepancy indicates that the formerly determined intrinsic electronic equilibrium constant, K_i^*, which is shown in Figure 4, requires a verification.

The intrinsic electronic equilibrium constant for TiO_2 was also reported by Baumard and Tani,[19] and Lee et al.[18] However, their equilibrium constants were derived using the disorder

TABLE 1: Concentrations of Electronic and Ionic Defects in Undoped TiO_2 within the Regimes Corresponding to Different Oxygen Activities and Governed by Simplified Charge Neutrality Conditions.[a]

regime charge neutrality	extremely reduced $n = 3[Ti_i^{\bullet\bullet\bullet\bullet}]$	strongly reduced $n = 2[V_O^{\bullet\bullet}]$	reduced $[V_O^{\bullet\bullet}] = 2[V_{Ti}^{\prime\prime\prime\prime}]$	oxidized $[V_O^{\bullet\bullet}] = 2[V_{Ti}^{\prime\prime\prime\prime}]$	strongly oxidized $p = 4[V_{Ti}^{\prime\prime\prime\prime}]$
defects					
n	$(3K_2)^{1/4}p(O_2)^{-1/4}$	$(2K_1)^{1/3}p(O_2)^{-1/6}$	$(K_i^4K_1/2K_3)^{1/6}p(O_2)^{-1/4}$	$(K_i^4K_1/2K_3)^{1/6}p(O_2)^{-1/4}$	$(K_i/4K_3)p(O_2)^{-1/5}$
p	$K_i(3K_2)^{-1/4}p(O_2)^{1/4}$	$K_i/(2K_1)^{1/3}\,p(O_2)^{1/6}$	$(2K_3K_i^2/K_1)^{1/6}\,p(O_2)^{1/4}$	$(2K_3K_i^2/K_1)^{1/6}(O_2)^{1/4}$	$(4K_3)^{1/5}\,p(O_2)^{1/5}$
$[V_{Ti}^{\prime\prime\prime\prime}]$	$3K_3K_2/K_i^4\,p(O_2)^0$	$(2K_1)^{4/3}\,K_3/K_i^4\,p(O_2)^{1/3}$	$(K_1^2K_3/4K_i^4)^{1/3}\,p(O_2)^0$	$(K_1^2K_3/4K_i^4)^{1/3}p(O_2)^0$	$(K_3/256)^{1/5}p(O_2)^{1/5}$
$[V_O^{\bullet\bullet}]$	$K_1(3K_2)^{1/2}p(O_2)^0$	$(K_1/4)^{1/3}p(O_2)^{-1/6}$	$(2K_1^2K_3/K_i^4)^{1/3}\,p(O_2)^0$	$(2K_1^2K_3/K_i^4)^{1/3}\,p(O_2)^0$	$[K_1(4K_3)^{2/5}/K_i^2]\,p(O_2)^{1/10}$
$[Ti_i^{\bullet\bullet\bullet\bullet}]$	$(K_2/27)^{1/4}\,p(O_2)^{-1/4}$	$K_2/2K_1\,p(O_2)^{-1/2}$	$(2K_2^2K_3/K_1)^{1/2}p(O_2)^{-1/4}$	$(2K_2^2K_3/K_1)^{1/2}\,p(O_2)^{-1/4}$	$[K_2(4K_3)^{3/5}/K_i^3]\,p(O_2)^{-2/5}$

[a] Equilibrium constants: K_1, K_2, K_3, and K_i are defined by eqs 5, 6, 7, and 8, respectively.

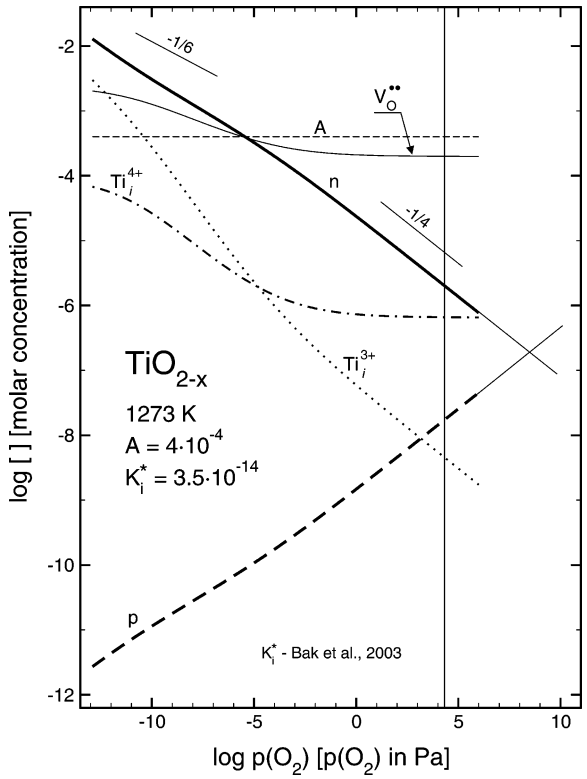

Figure 2. Defect diagram, representing the effect of $p(O_2)$ on the concentration of defects for TiO_2 at 1273 K and $A = 4 \times 10^{-4}$ for the intrinsic equilibrium constant, K_i^*, reported by Bak et al.[9]

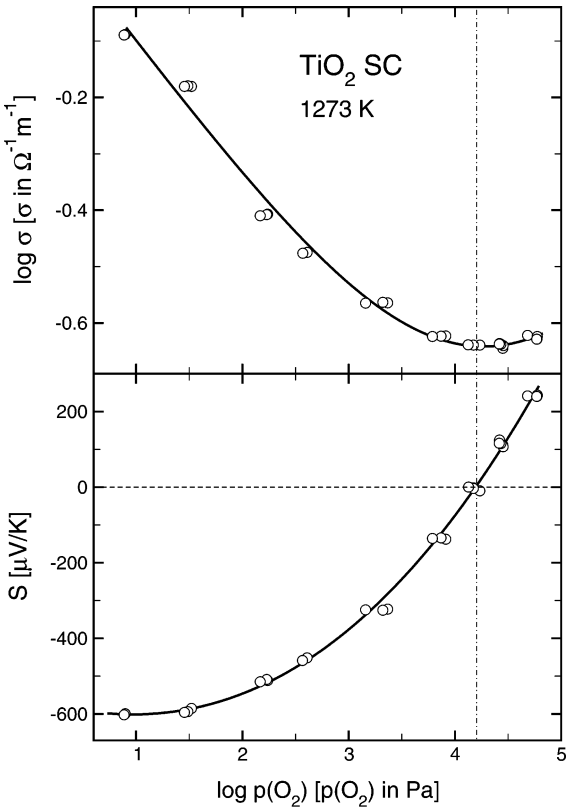

Figure 3. The effect of $p(O_2)$ on electrical conductivity[7] and thermoelectric power[7] for high purity TiO_2 single crystal determined at 1273 K.

model based on tetravalent Ti interstitials as the predominant defects. Since this model is inconsistent with the model derived in the present work, their equilibrium constants may not be used to assess the defect model derived in the present work that is based on oxygen vacancies as the predominant defects.

The purpose of the following section is the determination of the equilibrium constant K_i based on our own data of the electrical properties determined for well-defined TiO_2 single crystal,[7] and the thermogravimetry data reported in the literature.[12−18]

3. Equilibrium Constant K_i

3.1. First Approach. The equilibrium constant K_i may be determined from a relation between the electronic disorder and an experimentally measured property, such as nonstoichiometry.[12−18] Assuming that the predominant defects in TiO_2 are oxygen vacancies, the concentrations of both electronic and ionic defects are involved in the following charge neutrality:

$$n + A = p + 2[V_O^{\bullet\bullet}] \tag{15}$$

where A denotes the effective concentration of singly ionized acceptors, which is defined by eq 13. On the other hand, the deviation from stoichiometry, x in TiO_{2-x}, is determined by the deficit in oxygen sublattice and depends on the concentration of oxygen vacancies (the predominant defects). This concentration is a sum of two components:

(1) The concentration related to the amount of incorporated or released oxygen, according to the reaction expressed by eq 1. This process changes the O/Ti ratio

(2) The concentration related to the effective amount of incorporated acceptors, A, ($A = 2[V_O^{\bullet\bullet}]$). This process does not influence the O/Ti ratio

Consequently, x can be expressed by the concentration of oxygen vacancies and A as

$$x = [V_O^{\bullet\bullet}] - \frac{1}{2}A = \frac{1}{2}(n - p) \tag{16}$$

Therefore:

$$[V_O^{\bullet\bullet}] = x + \frac{1}{2}A \tag{17}$$

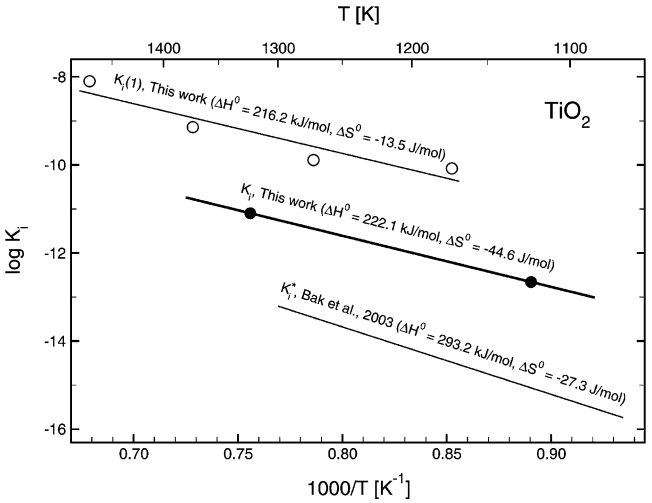

Figure 4. Intrinsic electronic equilibrium constant, K_i, for TiO_2 as a function of $1/T$ showing (1) the data reported by Bak et al.,[9] denoted as K_i^*; (2) the data determined in the first approach, denoted as $K_i(1)$; and (3) the data determined in the second approach, denoted as K_i.

From eq 16 we have

$$2x = n - p = n - \frac{K_i}{n} \tag{18}$$

The positive solution of the eq 18 is

$$n = x + \sqrt{x^2 + K_i} \tag{19}$$

Combination of eqs 5, 17, and 19 results in

$$\log p(O_2) = 2\log K_1 - 2\log\left(\frac{1}{2}A\right) - 4\log(x + \sqrt{x^2 + K_i}) \tag{20}$$

Since thermogravimetric data corresponds to the changes of mass related to the changes of nonstoichiometry x, rather than its absolute value, the deviation from stoichiometry should be expressed as $x + x^*$, where x^* is the reference level. The continuous lines in Figure 5 represent the best fit of the model expressed by eq 20 to the experimental data. The determined equilibrium constant K_1, along that reported by Kofstad,[12] is shown in Figure 6. The equilibrium constant K_i, denoted as $K_i(1)$, is shown in Figure 4 (the top line). The equilibrium constant $K_i(1)$ was used for the determination of new defect disorder, at 1273 K and $A = 4\cdot10^{-4}$, that is shown in Figure 7. As seen, the $n-p$ transition point in this case corresponds to substantially reduced $p(O_2)$ that is markedly lower than the experimental one shown in Figure 3 and represented by the vertical line. Consequently, one may expect that the optimal value of K_i, which is consistent with the experimental data, is between K_i^* and $K_i(1)$. This value will be determined using the second approach that is based on the data of electrical properties.

3.2. Second Approach. The equilibrium constant, K_i, in this approach is determined using the recently obtained self-confirmatory data of both electrical conductivity and thermopower vs $p(O_2)$ at different stages of prolonged oxidation at 1123 K,[8] which are shown in Figure 8. As seen, the $n-p$ transition point for "as grown" TiO_2 single crystal, indicated by the minimum of the electrical conductivity and the thermoelectric power assuming zero, corresponds to $p(O_2) = 8.3$ kPa. The prolonged oxidation (2500 h) results in a shift of the $n-p$ transition point to 0.7 kPa.[8] This point may be used for the determination of the equilibrium constant K_i, through derivation

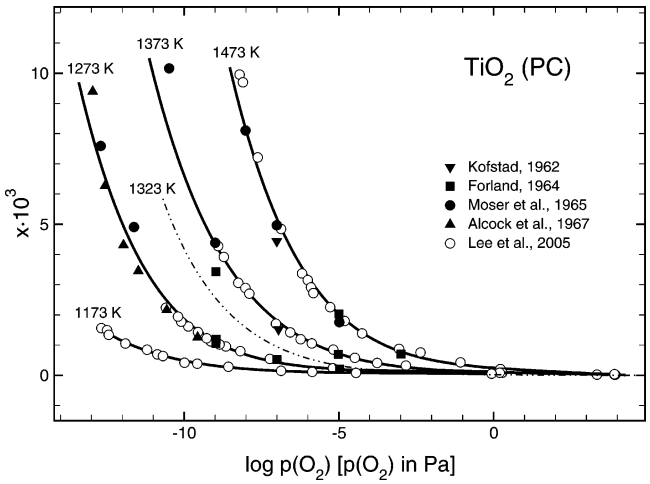

Figure 5. The deviation from stoichiometry, x, for TiO_2. The data points were determined from the thermogravimetry data[12−18] and the dashed line was determined by fitting the parameters K_i and A to achieve a consistency with the experimental data, including electrical conductivity, thermoelectric power, and the thermogravimetry.

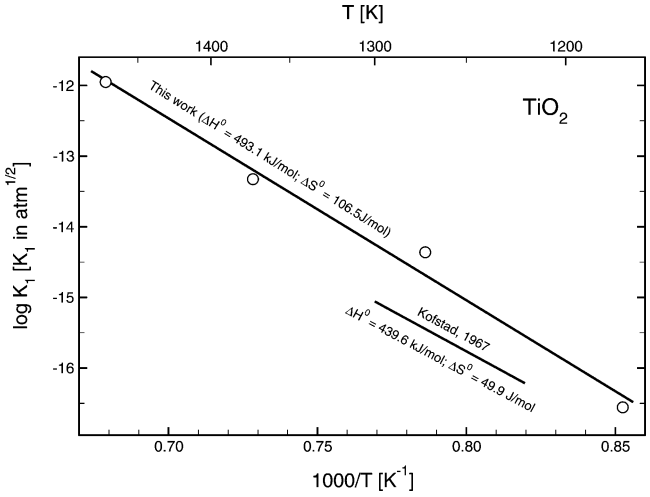

Figure 6. Equilibrium constant of the formation of oxygen vacancies, K_1, for TiO_2 as a function of $1/T$, determined in the present work along with that reported by Kofstad.[12]

of appropriate defect diagram, if the effective concentration of acceptors, A, is known. Its value may be determined from the data of thermoelectric power obtained during the prolonged oxidation of TiO_2 at 1123 K (Figure 9).

As seen in Figure 9, the prolonged oxidation of TiO_2 results in an increase of thermoelectric power from $+450$ μV/K for "as grown" single crystal to $+710$ μV/K. For p-type nondegenerated semiconductor the thermoelectric power, S, is the following function of the concentration of electron holes:

$$S = \frac{k}{e}\left(\ln\frac{N_V}{p} + A_p\right) \tag{21}$$

where k is the Boltzmann constant, e is elementary charge, N_V is the effective density of states in the valence band, and A_p is the kinetic constant, which depends on the way in which the holes mobility varies with energy in the band.[20] In the case of spherical symmetry of isoenergetic surface in the wave vector space, the density of states is as follows:

$$N_V = 2\left(\frac{2\pi m_p^* kT}{h^2}\right)^{3/2} \tag{22}$$

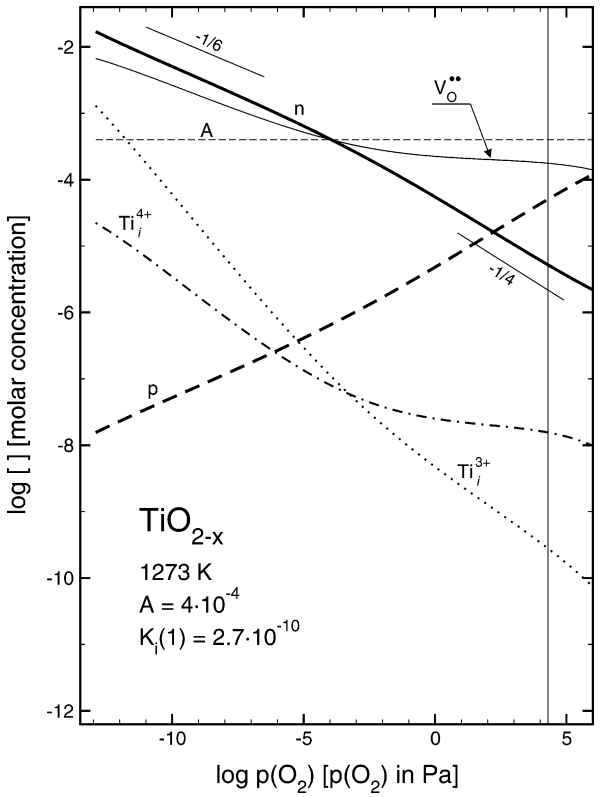

Figure 7. Defect diagram, representing the effect of $p(O_2)$ on the concentration of defects for TiO_2 at 1273 K and $A = 4 \times 10^{-4}$ for the intrinsic equilibrium constant $K_i(1)$ determined in the first approach using the data of thermogravimetry.[12−18]

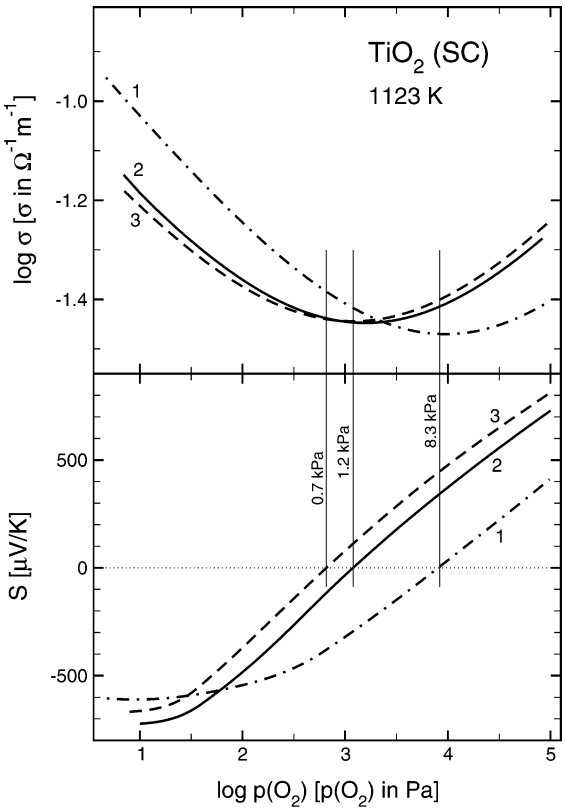

Figure 8. The effect of $p(O_2)$ on both electrical conductivity (upper part) and thermoelectric power (lower part) for high purity TiO_2 single crystal determined at 1123 K; the curve 1 represent these electrical properties in the Kinetic Regime I (within 20 h) and curves 2 and 3 represent the plots obtained after prolonged oxidation lasting 1500 and 2500 h, respectively (Kinetic Regime II).

where m_p^* is the effective mass of electron hole, T is absolute temperature, and h is the Planck constant. It is generally assumed that the valence band in TiO_2, originated from hybridization of 2p oribitals of oxygen atoms, is broad. Therefore, the effective mass of electron hole is expected to be very close to the mass of a single free electron, m_e. Assuming that the parameter A_p is substantially lower than the component $\ln(N_V/p)$, the concentration of electron holes is

$$p = 2\left(\frac{2\pi m_e kT}{h^2}\right)^{3/2} \exp\left(\frac{eS}{k}\right) \tag{23}$$

Assuming that the molar volume of TiO_2 is $1.89 \cdot 10^{-5}$ m^3, we have

$$p = 1.51 \cdot 10^{-6} \tag{24}$$

Consequently, the consistency between the experimental data and the defect disorder model requires that the value of the equilibrium constant K_i, and the effective concentration of acceptors, A, must be chosen in such a way that the determined defect disorder diagram at 1123 K exhibits the $n-p$ transition at $p(O_2) = 0.7$ kPa and, independently, the concentration of electron holes at $p(O_2) = 75$ kPa is equal to 1.51×10^{-6}. The iterative approach results in the following parameters:

$$K_i = 2.2 \times 10^{-13} \tag{25}$$

$$A = 4.8 \times 10^{-4} \tag{26}$$

The related defect diagram is shown in Figure 10. The filled point in this figure represents the concentration of electron holes at $p(O_2) = 75$ kPa, which corresponds to $m_p^* = 1\ m_e$.

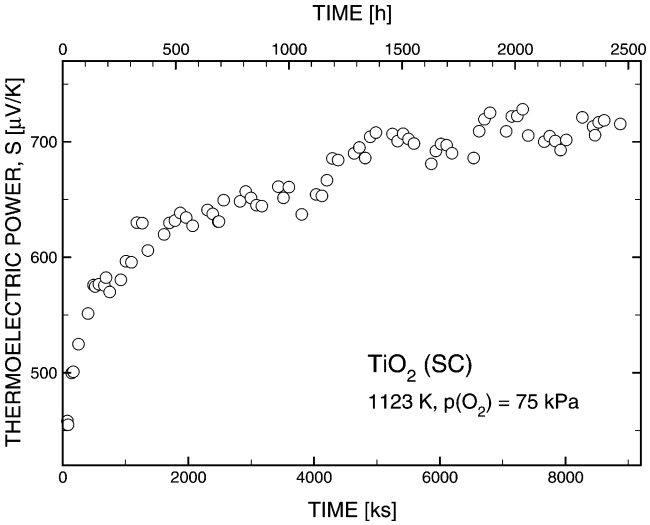

Figure 9. Changes of thermoelectric power, S, during prolonged oxidation of high purity TiO_2 single crystal at 1123 K and $p(O_2) = 75$ kPa.

The parameters K_i and A may also be determined at 1323 K using a similar procedure and based on the experimental data of thermoelectric power, before and after prolonged oxidation, shown in Figure 11. As seen, the $n-p$ transition point after long annealing (curve 2), at which $S = 0$, corresponds to $p(O_2) =$ 33.9 kPa. However, the data of S in Figure 11 may not be used for the determination of the concentration of electron holes because the S data at 1323 K and $p(O_2) = 75$ kPa correspond to the mixed regime, in which the electrical properties are

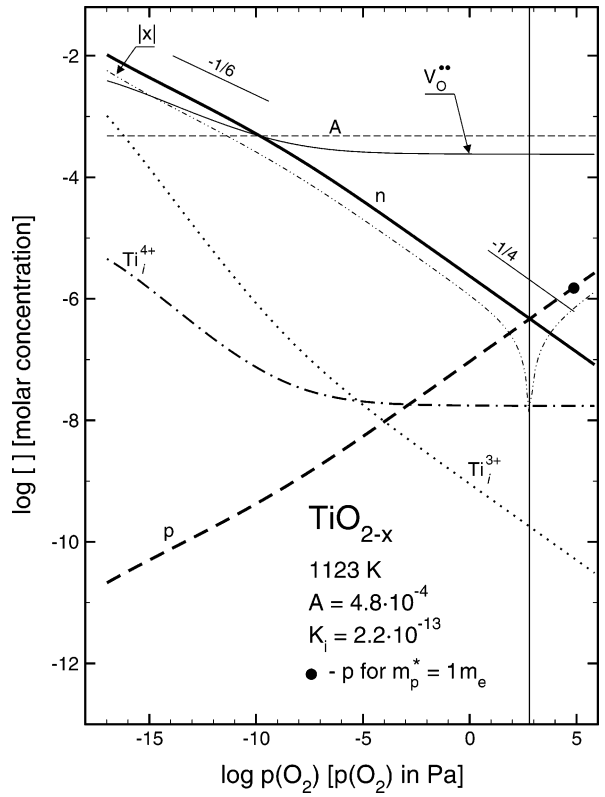

Figure 10. Defect diagram, representing the effect of $p(O_2)$ on the concentration of defects for TiO_2 at $A = 4.8 \cdot 10^{-4}$ and $K_i = 2.2 \cdot 10^{-13}$ for the intrinsic equilibrium constant determined in the second approach using the data of the electrical conductivity and thermoelectric power[7] at 1123 K; the filled point represents the concentration of electron holes determined at $m_p^* = 1\ m_e$.

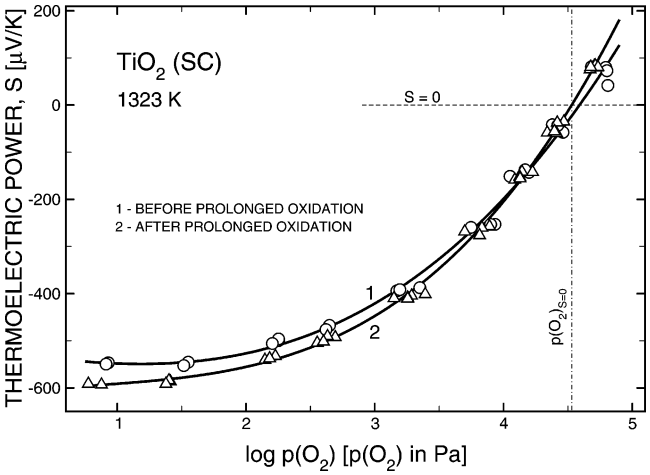

Figure 11. The effect of $p(O_2)$ on thermoelectric power for high purity TiO_2 single crystal at 1323 K, determined before and after prolonged oxidation at $p(O_2) = 75$ kPa.

determined by both charge carriers. Therefore, eq 23 may not be applied in this case; however, the parameter A may be determined from the data of the deviation from stoichiometry, x, which may be expressed as follows:[10]

$$x = \frac{2([Ti_i^{\bullet\bullet\bullet}] + [Ti_i^{\bullet\bullet\bullet\bullet}] - [V_{Ti}''''] + [V_O^{\bullet\bullet}]}{1 + [Ti_i^{\bullet\bullet\bullet}] + [Ti_i^{\bullet\bullet\bullet\bullet}] - [V_{Ti}'''']} \quad (27)$$

For a high purity TiO_2, the concentration of Ti vacancies is 4 times smaller than the effective concentration of acceptors, as it is represented by eq 14. However, as seen in Figure 5 the experimental data of the deviation from stoichiometry, x, are not available at 1323 K. Since the data in Figure 5 exhibit a regular pattern, one should expect that the data at 1323 K will be inbetween the data at 1273 and 1373 K. Using an iterative approach, the parameters K_i and A were selected to achieve the $n-p$ transition at $p(O_2) = 33.9$ kPa. At the same time, the deviation from stoichiometry, determined using eq 27, must be in the range inbetween the values corresponding to 1273 and 1373 K. The latter dependence is indicated by the dashed line in Figure 5. The resulting defect diagram, that is shown in Figure 12, was derived using the following parameters:

$$K_i = 8.0 \times 10^{-12} \quad (28)$$

$$A = 5.5 \times 10^{-3} \quad (29)$$

The three filled points in Figure 12 represent the concentrations of electrons determined within the n-type regime from the thermopower data for reduced TiO_2 shown in Figure 11 at $p(O_2) = 10$ Pa, assuming the following three possible values for the effective mass of electrons m_n^*: 1 m_e, 2 m_e, and 3 m_e. As seen, the value 2 m_e is consistent with the experimental data. This value suggests that the conduction band is narrower than the valence band or, alternatively, that electrons are transported according to the hopping mechanism.

The determined equilibrium constants K_i at 1123 and 1323 K, expressed by eqs 25 and 28 lead to the temperature dependence of electronic equilibrium constant, denoted as K_i, that is shown in Figure 4.

4. Band Gap

When the Maxwell-Boltzmann statistics applies to both electrons and electron holes, the equilibrium constant K_i may be related to the band gap, eg.,

$$K_i = N_V N_C \exp\left(-\frac{E_g}{kT}\right) \quad (30)$$

Assuming, according to eq 22, that

$$N_{V,C} = \text{const} \cdot T^{3/2} \quad (31)$$

we have

$$K_i = \text{const} \cdot T^3 \exp\left(-\frac{E_g}{kT}\right) \quad (32)$$

Taking into account the data shown in Figure 4, the band gap in the temperature range 1123−1323 K is equal to 2.0 eV.

It has been generally assumed that the band gap exhibits a linear change with temperature:[9]

$$E_g = E_g^{\,0} - \beta T \quad (33)$$

Taking into account that the average band gap value at room temperature is $E_g^0 = 3.0$ eV[9] and $\beta = 0.8$ meV/K,[19,21,22] there is a good agreement between the band gap determined in the present work and the band gap values reported in the literature.

5. Concentration of Titanium Vacancies

The effective concentrations of acceptors, A, that were used for derivation of defect disorder diagrams in Figures 10 and 12, correspond to high purity TiO_2 specimen after prolonged oxidation at 75 kPa. Therefore, according to eq 14 these values may be considered in terms of the concentration of Ti vacancies

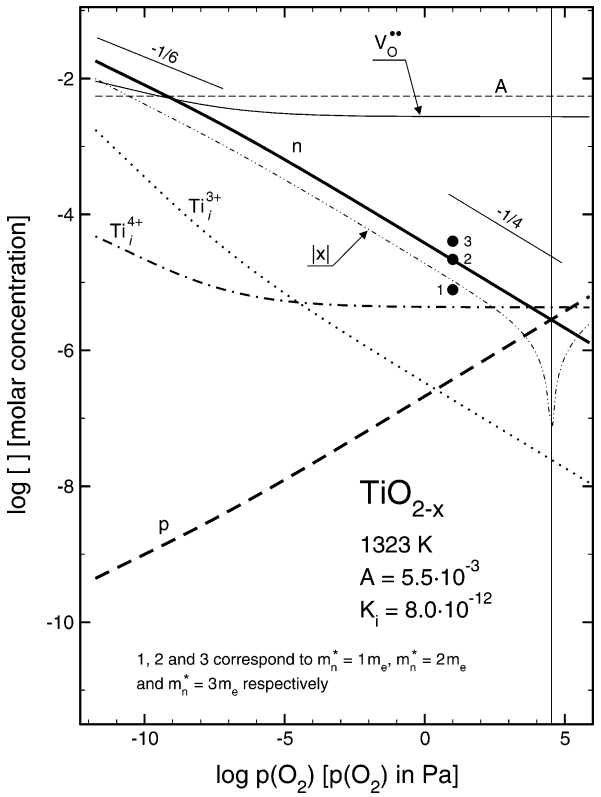

Figure 12. Defect diagram, representing the effect of $p(O_2)$ on the concentration of defects for TiO_2 at $A = 5.5 \times 10^{-3}$ and $K_i = 8 \times 10^{-12}$ for the intrinsic equilibrium constant determined in the second approach using the data of thermogravimetry[12−18] at 1323 K; the filled points represent the concentration of electrons calculated for $m_n^* = 1$, 2, and $3m_e$ (denoted by 1, 2, and 3, respectively).

corresponding to the gas/solid equilibrium. According to the defect diagram based on simplified charge neutrality (shown in Figure 1), the concentrations of both Ti vacancies and oxygen vacancies in the Reduced Regime are practically independent of $p(O_2)$. Then

$$2[V_{Ti}''''] = [V_O^{\bullet\bullet}] \tag{34}$$

As seen in Table 1, the concentration of Ti vacancies in this regime is

$$[V_{Ti}''''] = \left(\frac{K_3 K_1^{\,2}}{4K_i^{\,4}}\right)^{1/3} \tag{35}$$

where K_1 and K_3 are expressed by eqs 5 and 7, respectively. Therefore

$$K_3 = \frac{K_i^{\,4} A^3}{16 K_1^{\,2}} \tag{36}$$

Figure 13 represents the equilibrium constant K_3 that was determined using the constants K_i, K_1, and A determined at 1123 and 1323 K. This equilibrium constant was used for the determination of equilibrium values of the concentration of Ti vacancies, that are shown by the solid line in Figure 14 (Kinetic Regime II).

To estimate the concentrations of Ti vacancies in the Kinetic Regime I, the dependence between the effective concentration of acceptors, A, and the $p(O_2)$ at the $n-p$ transition, $p(O_2)_{n=p}$, was determined. These data, plotted in terms of $\log[V_{Ti}'''']$ vs $\log p(O_2)_{n=p}$, are shown in Figure 15. These calibration lines were used for determination of the concentration of Ti vacancies before the prolonged oxidation (Kinetic Regime I). This regime

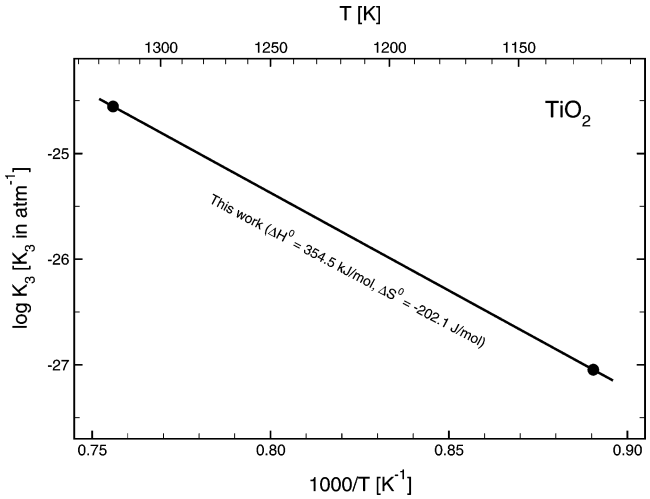

Figure 13. Equilibrium constant of the formation of Ti vacancies, K_3, for TiO_2 as a function of $1/T$, determined in the present work.

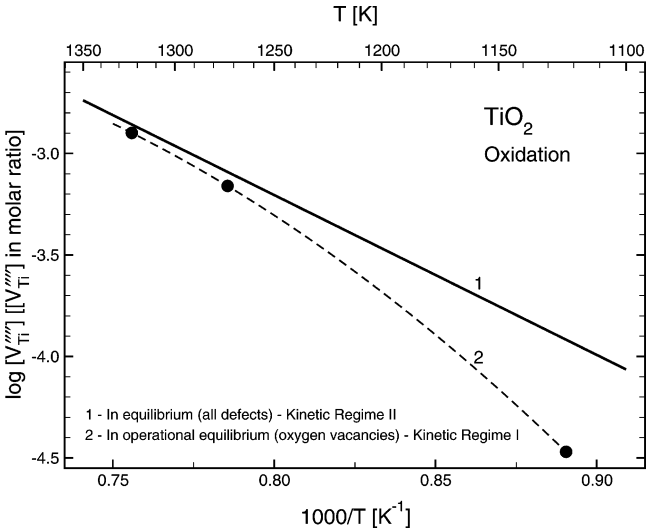

Figure 14. Concentration of Ti vacancies as a function of $1/T$; solid line corresponds to equilibrium (Kinetic Regime II) and dashed line corresponds to the operational equilibrium (Kinetic Regime I).

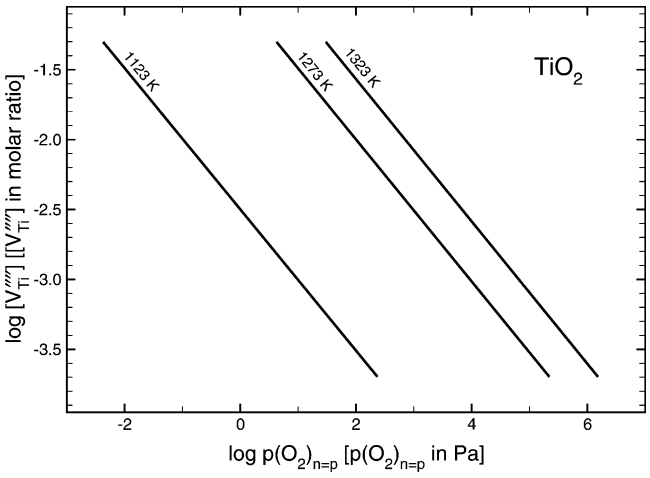

Figure 15. Isothermal dependencies between the concentration of Ti vacancies and the oxygen activity corresponding to the $n-p$ transition, $p(O_2)_{n=p}$.

corresponds to the annealing within 10−20 h when the fast defects (oxygen vacancies and Ti interstitials) reach equilibrium, while the Ti vacancies do not correspond to equilibrium due to the kinetic reason. The dashed line in Figure 14 represents the nonequilibrium concentration of Ti vacancies, determined according to eq 14, in the Kinetic Regime I. The distance between the two lines in Figure 14 is representative of the difference in the concentration of Ti vacancies between their equilibrium concentration, that may be established only after prolonged oxidation lasting several thousand hours (Kinetics Regime II),[8] and their nonequilibrium concentrations that may usually be established during commonly applied experimental conditions for the determination of electrical properties.

6. Conclusions

The present work determined defect disorder diagram for undoped TiO_2 in terms of the effect of oxygen activity on the concentration of both electronic and ionic defects. This diagram explains amphoteric properties of TiO_2 in terms of both oxygen vacancies, that are the predominant ionic defects within a wide range of $p(O_2)$, and Ti interstitials. The diagram was derived at a constant term A, representing the concentration of Ti vacancies, because A remains practically constant during commonly applied experimental conditions at elevated temperatures (Kinetic Regime I).

This work shows that the concentration of Ti vacancies in TiO_2 in the Kinetic Regime I, differs from their equilibrium concentration (Kinetic Regime II). The latter may only be achieved after prolonged oxidation. The derived defect disorder diagram may be used for the selection of optimized processing conditions in order to obtain TiO_2 with well-defined defect disorder and the related semiconducting properties.

Acknowledgment. The present work was supported by the Australian Research Council, Rio Tinto Ltd., Brickworks Ltd., Mailmasters Pty. Ltd., Sialon Ceramics Pty., and Avtronics (Australia) Pty. Ltd. This work was performed within the research and development program on solar-hydrogen.

References and Notes

(1) Fujishima, A.; Honda, K. *Nature* **1972**, *238*, 37.
(2) Nowotny, J.; Sorrell, C. C.; Bak, T.; Sheppard, L. R. In: *Materials for Energy Conversion Devices*; Woodhead: Cambridge, 2005; pp 84−116.
(3) Nowotny, J.; Sorrell, C. C.; Sheppard, L. R.; Bak, T. *Int. J. Hydrogen Energy* **2005**, *30*, 521.
(4) Nowotny, J.; Sorrell, C. C.; Bak, T.; Sheppard, L. R. *Adv. Sol. Energy*, in print.
(5) Kofstad, P. *Nonstoichiometry, Diffusion and Electrical Conductivity of Binary Metal Oxides*; Wiley: New York, 1972.
(6) Matzke, Hj. In: *Nonstoichiometric Oxides*; Sorensen, O. T., Ed.; Academic Press: New York, 1981; pp 156−231.
(7) Nowotny, M. K.; Bak, T.; Nowotny, J. *J. Phys. Chem. B* **2006**, *110*, 16270.
(8) Nowotny, M. K.; Bak, T.; Nowotny, J.; Sorrell, C. C. *Phys .Status Solidi*, **2005**, *242*, R88.
(9) Bak, T.; Nowotny, J.; Rekas, M.; Sorrell, C. C. *J. Phys. Chem. Solids* **2003**, *62*, 1043.
(10) Bak, T.; Nowotny, J.; Rekas, M.; Sorrell, C. C. *J. Phys. Chem. Solids*, **2003**, *64*, 1057.
(11) Nowotny, M. K.; Bak, T.; Nowotny, J. *J. Phys. Chem. B* **2006**, *110*, 16283.
(12) Kofstad, P. *J. Less Common Metals* **1967**, *13*, 635,
(13) Kofstad, P. *J. Phys. Chem. Solids* **1962**, *23*, 1579.
(14) Frland, K. S. *Acta Chem. Scand.* **1964**, *18*, 1267.
(15) Moser, J. B.; Blumenthal, R. N.; Whitmore, D. H. *J. Am. Ceram. Soc.* **1965**, *48*, 384.
(16) Atlas, L. M.; Schlehman, G. J. reported by Moser J. B. et al. in *J. Am. Ceram. Soc.* **1965**, *48*, 384.
(17) Alcock, C. B.; Zador, S.; B. Steele, C. H. *Proc. Br. Ceram. Soc.* **1967**, *8*, 231.
(18) Lee, D.-K.; Jeon, J.-I.; Kim, M.-H.; Choi, W.; Yoo, H.-I. *J. Solid State Chem.* **2005**, *178*, 185.
(19) Baumard, J.-F.; Tani, E. *Phys. Status Solidi* **1977**, *39*, 373.
(20) Nowotny, J. In: *The CRC Handbook of Solid-State Electrochemistry*; Gellings, P. J., H. Bouwmeester, J. M., Eds.; CRC: Boca Raton, FL 1997; pp 121−159.
(21) Yahia, J. *Phys. Rev.* **1963**, *130*, 1711.
(22) Bube, R. H. In: *Photoconductivity of Solids*; Wiley: New York, 1966; p 237.